Optik - International Journal for Light and Electron Optics 178 (2019) 190–196

Contents lists available at ScienceDirect

Optik

journal homepage: www.elsevier.com/locate/ijleo

Original research article

Theoretical study on thermal characteristic of MgO: PPLN crystal in high power optical parametric oscillator

Kuo Zhang[a,b,*], Fei Chen[a,b], Qikun Pan[a,b], Deyang Yu[a,b], Yang He[a,b]

[a] State Key Laboratory of Laser Interaction with Matter, Changchun Institute of Optic, Fine Mechanic and Physics, Chinese Academy of Sciences, Changchun, China

[b] Innovation Laboratory of Electro-optical Countermeasures Technology, Changchun Institute of Optic, Fine Mechanic and Physics, Chinese Academy of Sciences, Changchun, China

ARTICLE INFO

Keywords:
Optical parametric oscillator
MgO: PPLNCrystal
Temperature distribution
Contacting surface topography
Heat transfer

ABSTRACT

This study focuses on the thermal characteristic of an end-pumped MgO: PPLN crystal by solving the transient temperature evolution model in a high power optical parametric oscillator. In this model, an approach based on contact mechanics theory is proposed to quantitatively calculate the heat transfer between rough contacting surfaces of crystal and heat sink. Based on the model, a parametric study has been performed to investigate the influence of the heat sink property, pump laserand crystal dimension on the thermal characteristic of the laser crystal. Obtained results reveal a closed correlation between the mentioned parameters and the thermal characteristic of the crystal indicating that a proper selection of the parameters is essential to control the crystal temperature and improve the performance of the laser.

1. Introduction

The output of mid-infrared (3–5 μm) lasers exhibits good optical transmission through atmosphere, which is widely prospected used in spectroscopy, environmental monitoring, optical communication and optical coherence tomography [1–4]. Quasi-phase-matched optical parametric oscillators (OPO) based on MgO-doped periodically poled lithium niobate (MgO: PPLN) crystal is the particularly attractive solution to obtain the mid-infrared laser output due to the high nonlinear coefficient, wide optical transparency range and tunable characteristics of MgO: PPLN crystals [5–7]. Heat generation due to absorption of pump laser in crystal will cause the temperature gradient in the gain medium, which will lead to undesirable phenomena, such as thermal lensing and stress birefringence. These effects will degrade the optical properties of the crystal, reduce the laser beam quality and overall conversion efficiency [8,9]. Therefore, study on the thermal characteristic of MgO: PPLN crystal is essential to control these adverse phenomena and their subsequent effects on laser beam quality and conversion efficiency.

Heat generated in laser crystal is a transient process which is related with the laser irradiating time and complicated heat dissipate boundary conditions, therefore, numerical simulation approach is adopted by some researchers to investigate the temperature distribution of Nd: YVO_4 crystal in diode-pumped solid-state lasers [10–14]. These researches provide a valid method to study the thermal characteristic of crystal with complicated boundary conditions and variable physics properties. Although the absorption of laser for MgO: PPLN crystal is much less than Nd: YVO_4 crystal, the thermal phenomena, such as thermal dephasing, has also been experimentally observed in MgO: PPLN crystal for the laser input power ≥10 W [15,16].For crystal temperature is related with output wavelength of OPO, MgO: PPLN crystal is mounted into heat sink to maintain crystal temperature at a constant value. Crystal

* Corresponding author.
E-mail address: cole_fx@163.com (K. Zhang).

https://doi.org/10.1016/j.ijleo.2018.09.138
Received 24 July 2018; Accepted 24 September 2018

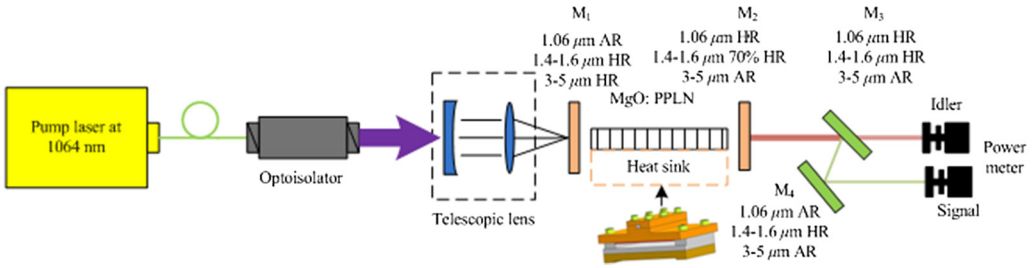

Fig. 1. Configuration of a MgO: PPLN crystal based OPO pumped by Yb-fiber laser.

and heat sink mutually transfer heat and finally reach thermal balance state when OPO operates stable. However, as far as our knowledge, no research has focused on the numerical approach to simulate the thermal characteristic of crystal and heat sink synchronously in OPO.

In this paper, a transient heat transfer model is proposed to calculate temperature distribution of MgO: PPLN crystal in high power OPO. The heat transfer between the crystal and heat sink is quantitatively calculated using contact mechanics theory. Numerical simulation is employed to investigate the correlation between thermal characteristic of laser crystal and the parameters, such as heat sink property, pump laser and crystal dimension. The obtained result is essential for determining the appropriate parameters to optimize the performance of high power OPO.

2. Theoretical model

Fig. 1 shows the configuration of a typical OPO comprising pump laser, optoisolator, telescopic lens, laser resonant and output mirrors. The pump source is an Yb-fiber laser providing 30 W of the average power with TEM_{00} mode at the wavelength of 1.064 μm. The collimated output beam from the Yb-fiber pump source passes through a pair of telescopic lenses and is focused into the MgO: PPLN crystal. The OPO is configured in a double path single resonator cavity composed of two plane reflectors M_1 and M_2, the parameters of which are listed in detail in Fig. 1. The dimensions of MgO: PPLN crystal is 50 mm × 3 mm × 2 mm, which is mounted in a copper heat sink (the three-dimensional structure of heat sink is shown in Fig. 1).

During the laser operation, the pump laser and signal laser irradiate at the ends of the crystal in the resonant. Therefore, a portion of the pump laser power and signal laser power deposit in the crystal resulting in the temperature distribution $T(x, y, z)$, which satisfies the partial differential equation:

$$\rho C_p \frac{\partial t}{\partial \tau} = \frac{\partial}{\partial x}\left(k\frac{\partial t}{\partial x}\right) + \frac{\partial}{\partial y}\left(k\frac{\partial t}{\partial y}\right) + \frac{\partial}{\partial z}\left(k\frac{\partial t}{\partial z}\right) + Q(x, y, z) \tag{1}$$

Where ρ, C_p and k are, respectively, the density specific heat capacity and heat conductivity of the crystal. Q(x, y, z) represents the thermal source generation due to the absorption of laser with Gaussian distribution, which can be described as [10,11]:

$$Q(x, y, z) = \eta_h P_{in} p(x, y, z) \frac{\alpha_T}{1 - e^{-\alpha_T L}} e^{-\alpha_T z} \tag{2}$$

$$p(x, y, z) = \frac{2}{\pi\omega_p^2} e^{-\frac{2(x^2+y^2)}{\omega_p^2}} \tag{3}$$

$$\omega_p^2(z) = \omega_{p0}^2 \left\{1 + \left[\frac{M\lambda_p z}{\pi n_0 \omega_{p0}^2}\right]^2\right\} \tag{4}$$

Where, $p(x, y, z)$ is normalized laser radiation distribution; P_{in} is the total incident laser power; L is the length of the crystal; α_T is absorption coefficient; ω_p is the radius of laser beam at the incident surface; ω_{p0} is the waist radius of the incident beam, λ_p is the wavelength of incident beam; n_0 is refractive index of crystal; M^2 is beam quality factor of the incident beam; η_h is the fraction of incident laser power converted to heat, for MgO: PPLN crystal, the value of η_h is reasonably set to 0.3 [17,18]. It should be noted that the thermal source Q is sum of the heat generated in MgO: PPLN crystal due to the absorption of pump laser and signal laser.

The heat flux normal to each surface of the laser crystal is proportional to the temperature rise of that surface. The heat transferred between the crystal and heat sink can be expressed as:

$$\Delta q_1 = h_H(t_H - t) \tag{5}$$

Where t_H is the temperature of heat sink, h_H is the equivalent heat transfer coefficient, which is related with the thermal and mechanical properties of crystal and heat sink. According to Cooper-Mikic-Yovavoich model in contact mechanics theory, the equivalent heat transfer coefficient can be expressed as [19]:

$$h_H = \frac{k_s}{2\sqrt{2\pi}}\frac{m}{\sigma}\frac{\exp(-\lambda^2/2)}{[1-\sqrt{0.5(\mathrm{erfc}(\lambda/\sqrt{2}))}]^{1.5}} \tag{6}$$

Where, k_s is the average value of heat conductivity of crystal and heat sink, m is the average slope of contacting surface roughness, σ is the square root of contacting surface roughness, λ is the function of contacting pressure P and contacting material hardness H_m, which can be expressed as:

$$\lambda = \sqrt{2}\,\mathrm{erfc}^{-1}\left(\frac{2P}{H_m}\right) \tag{7}$$

Where, erfc represents the compensation error function. The laser incidence surfaces and exterior faces of heat sink have natural heat conversion with surrounding air, the natural heat transfer coefficient is quoted as 3 W/(m^2·K) [18].

3. Numerical simulations and discussions

Effects of various parameters, including heat sink property, pump laser characteristics and dimension of crystal have been analyzed in the following sections. The temperature distribution along optical axis in crystal is a critical parameter to evaluate the crystal thermal characteristic. Therefore, the analysis is performed by considering the variation of temperature distribution versus the mentioned parameters.

3.1. Heat sink property

In this section, the influence of heat sink property such as: thermal and mechanical performance of material and contacting surface topography is analyzed, related parameters are list in Table 1.

The heat sink is heat up to 338 K to obtain the output laser wavelength of 3.8 μm, the pump laser power is 30 W provided by a fiber laser with 1064 nm wavelength. Fig. 2 illustrates the change of crystal temperature distribution with or without heat sink. The temperature of crystal increases continuously without heat sink. When the crystal is mounted in the heat sink, temperature increases dramatically at the initial period, then the crystal and heat sink reach the thermal balance state after the laser operates for 10 s. At this time, the temperature of crystal and heat sink is 338.8 K and 338.4 K respectively, there is nearly 0.55 K difference between crystal and heat sink is at the thermal balance state.

Heat transfer between crystal and heat sink is related with the thermal and mechanical properties and contacting surface topography, including contacting pressure, heat sink material, square root or surface roughness and slope of surface roughness. Contacting pressure represents the force applied to heat sink to compact the heat sink onto crystal. Heat sink material has different thermal and mechanical performance, which will lead to different thermal characteristic of crystal. Square root of surface roughness and slope of surface roughness are used to describe the contacting surface topography. The influence of mentioned parameters is numerically analyzed in Fig. 3. Fig. 3(a) illustrates that the crystal temperature will decrease as the contacting pressure increase. The increased contacting pressure makes crystal tightly contact with the heat sink, hence the temperature difference between crystal and heat sink become small. However the influence of contacting pressure is weak, the temperature is 0.1 K between the contacting pressure of 1 kPa and 10 kPa. Fig. 3(b) describes the temperature difference of different heat sink material. We compare the crystal temperature distribution with two kinds of heat sink made of aluminum and copper respectively. The result indicates that the crystal temperature with aluminum heat sink is a little higher than that with copper heat sink at thermal balance state, the temperature difference is nearly 2 K. Fig. 3(c) and (d) illustrate the influence of contacting surface topography on crystal temperature. Square root of surface roughness describes the surface roughness height, and slope of surface roughness describes the surface roughness pattern. As shown in Fig. 3(c), crystal temperature rises with the increase of square root of surface roughness increases, there is 1 K difference between the square root of surface roughness of 1 μm and 10 μm. The temperature distribution at cross section is nearly Gaussian pattern, there is 0.4 K difference between crystal center and crystal edge. However the influence of slope of surface roughness is much less than square root of surface roughness, the temperature decreases 0.5 K from the slope of surface roughness of 0.2 to 0.8.

3.2. Pump laser characteristic

The laser power deposition in crystal is the key factor to raise crystal temperature. The pump laser characteristics, including laser power and beam spot size are directly related to the power deposition in crystal.

Table 1
Thermal and mechanical performance of material and contacting surface topography.

	Thermal conductivity W/(m·K)	Material Density Kg/m3	Heat capacity J/(kg·K)	Contacting Hardness kgf/mm^2	Surface roughness μm	Surface roughness slope /
MgO: PPLN crystal	4.4	4650	640	630		
Copper heat sink	400	8960	385		1	0.4
Aluminum heat sink	201	2700	900		1	0.4

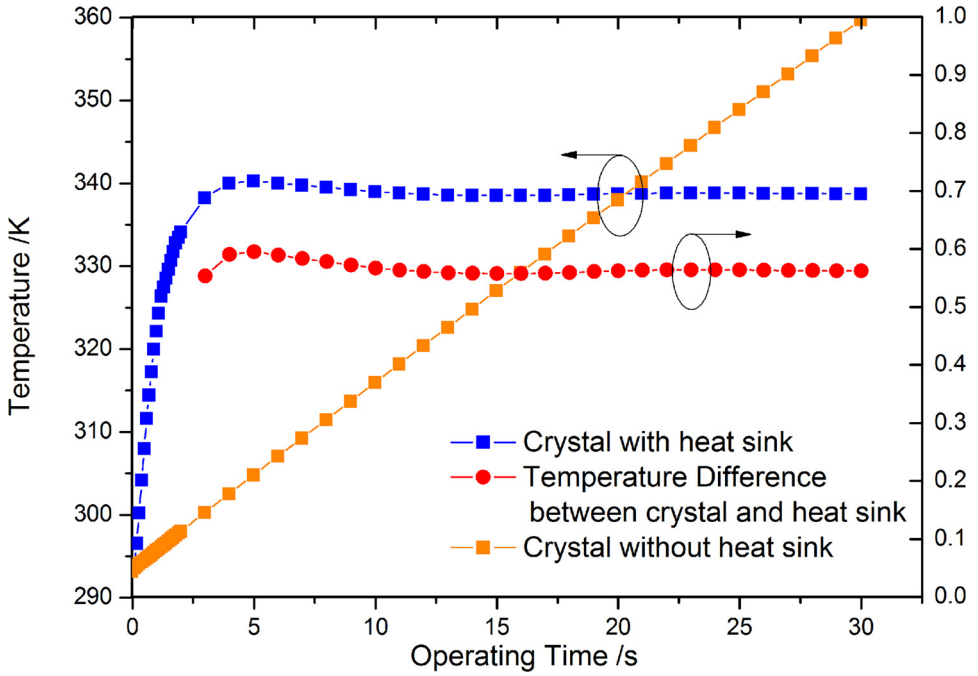

Fig. 2. Temporal evolution of crystal temperature versus heat sink.

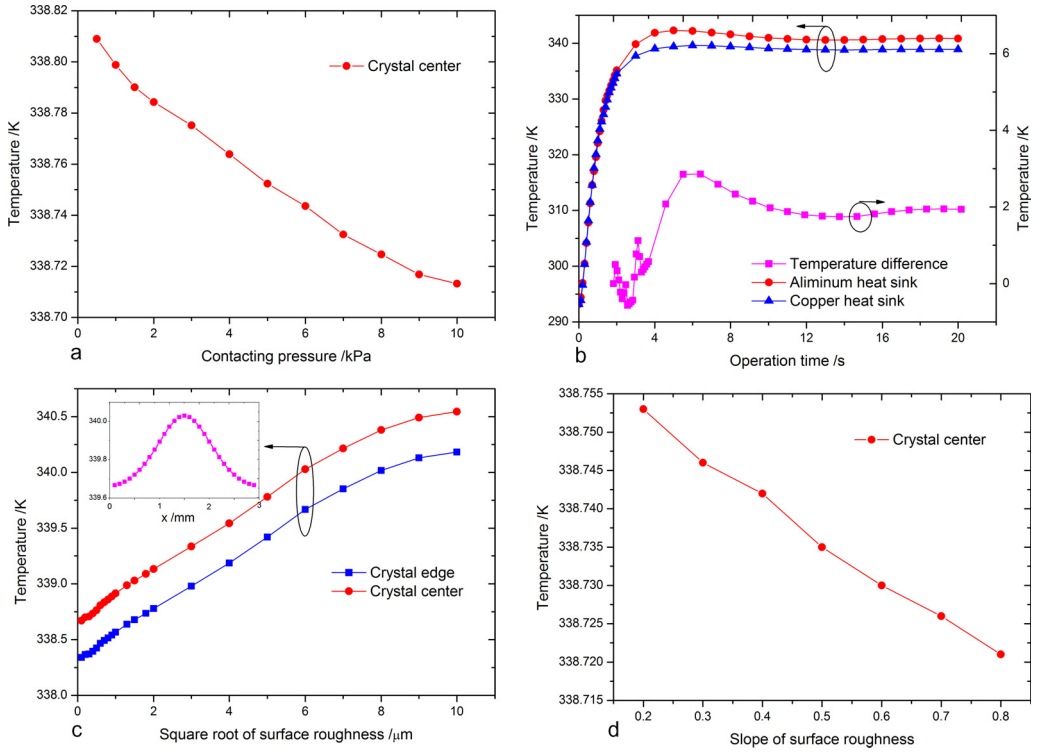

Fig. 3. Influence of thermal and mechanical properties and contacting surface topography: (a) Contacting pressure, (b) Heat sink material, (c) Square root of surface roughness and (d) Slope of surface roughness.

Fig. 4(a) illustrates the crystal temperature variation versus pump laser power. The temperature of crystal increases linearly with the pump power. For the condition of copper heat sink, the temperature is 340.75 K at 100 W pump power, which is 1.85 K higher than the condition of 30 W pump power. Crystal temperature variation with aluminum heat sink has the same trend with that with copper heat sink, however, the crystal temperature with aluminum heat sink is higher than that with copper heat sink at the same

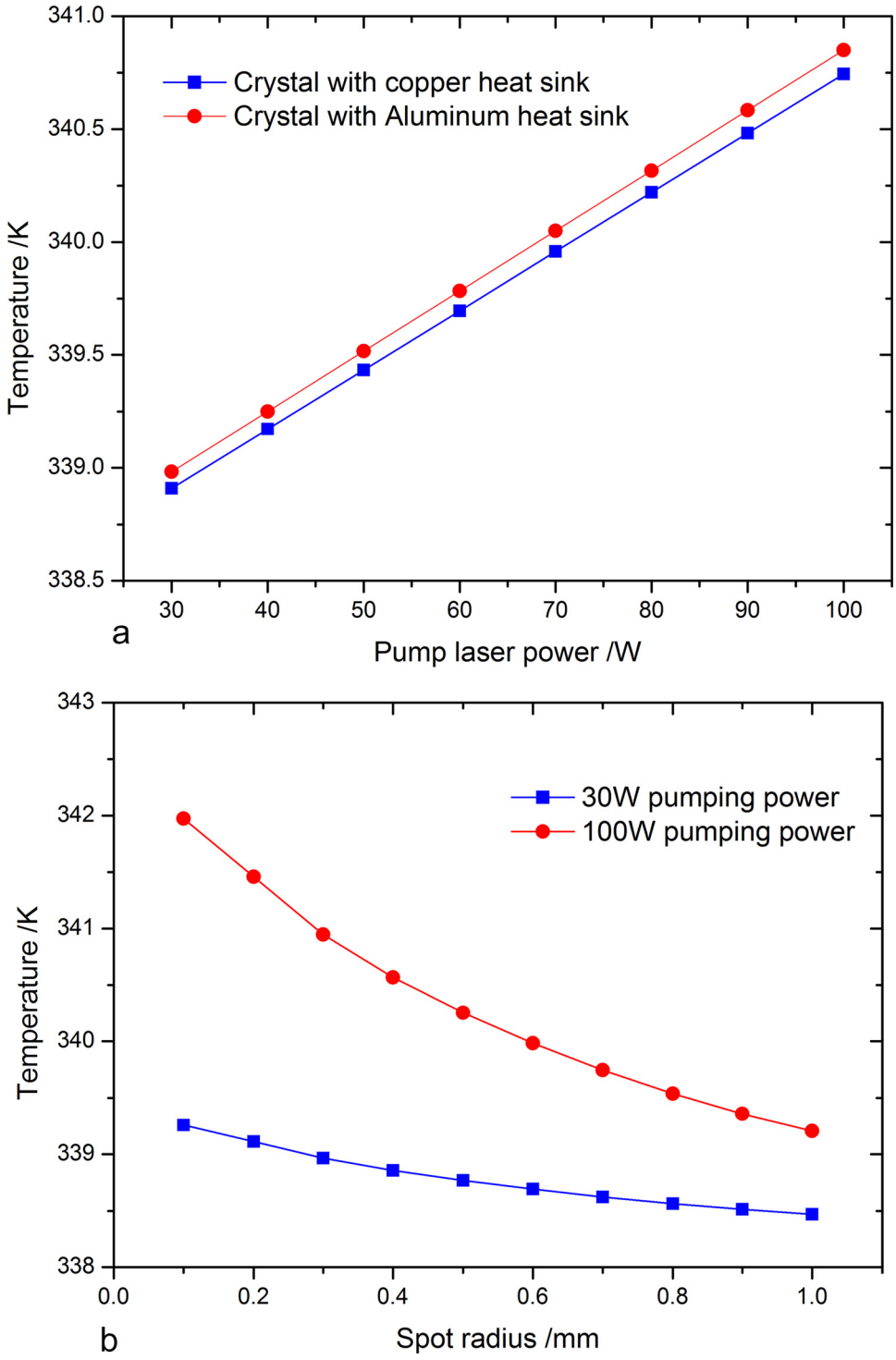

Fig. 4. Crystal temperature variation versus pump laser characteristic: (a) pump laser power and (b) beam spot radius.

pump power. Fig. 4(b) illustrates the crystal temperature variation versus spot radius at 30 W pump laser power and 100 W pump laser power respectively. It is obvious that this temperature decreases by enlarging the spot radius from 0.1 mm up to 1 mm, the difference of temperature is nearly 0.8 K at 30 W pump power condition, the value reaches 2.7 K at 100 W pump power condition.

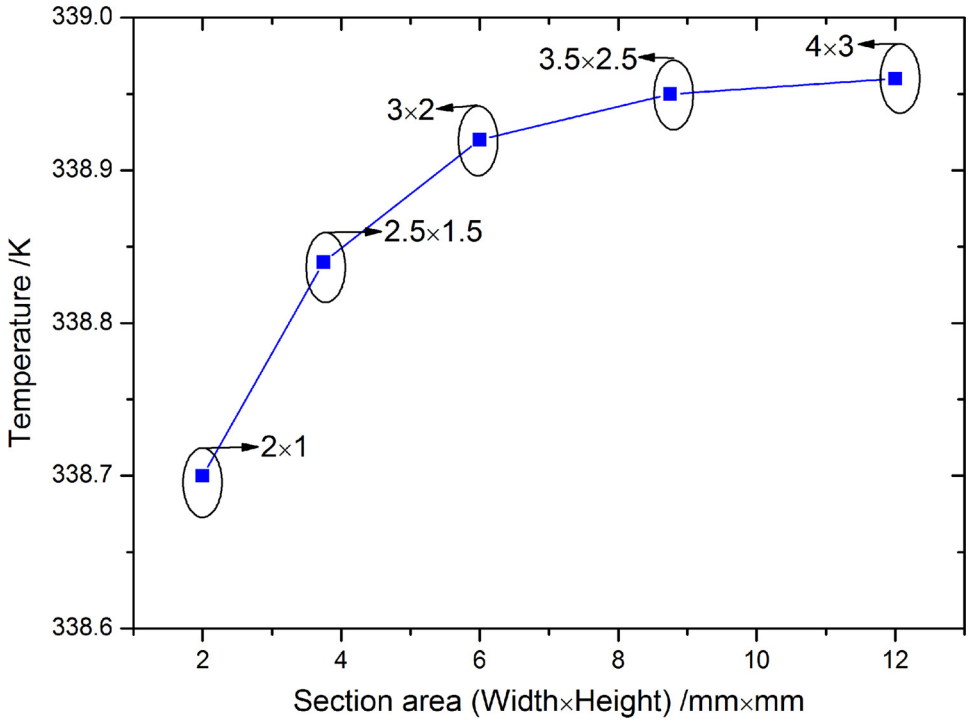

Fig. 5. Crystal temperature variation versus crystal dimension.

3.3. Crystal dimension

Crystal dimension is essential to affect the performance and cost of the laser. The crystal length is determined for certain OPO resonance structure, it is practical significance to study the influence of crystal sectional area on laser thermal characteristic.

Fig. 5 shows the temperature evolution of crystal for five different kinds of crystal sectional area typically stimulated for a pumping with 30 W power and 0.35 mm radius.The sectional areas of heat sink have fixed proportion with crystal sectional areas to avoid the influence of heat sink. It can be seen from Fig. 5 that the temperature raises with the enlargement of crystal sectional area, the temperature increment between sectional are of 2 mm^2 and 12 mm^2 is nearly 0.25 K. Therefore, under the premise of OPO normal function, it is optimized to adopt the crystal with small sectional area.

4. Conclusions

Thermal characteristic of MgO: PPLN crystal in a high power OPO is theoretically and numerically studied. A contact mechanical theory is introduced in this paper to quantitatively calculate the heat transfer between the crystal and heat sink. Temperature distribution can be numerically obtained by solving the transient heat transfer model modified according to the OPO structure. Correlation between thermal characteristic of laser crystal and various laser parameters has been investigated, the results of which are briefly explained in the following summary:

1 Heat sink conspicuously affects the crystal temperature. Crystal temperature will reach a thermal balance state with heat sink after the laser operation for a certain time. The influence of heat sink material and contacting surface topography has been numerically analyzed, the square root of surface roughness and heat sink material have obvious effect on crystal temperature.
2 Study on the influence of pump laser characteristic indicates that crystal temperature will rise with the increase of pump laser power or decrease of beam spot radius.
3 Crystal temperature will increase with the enlargement of crystal sectional area, which indicates that it is optimized to adopt a crystal with small sectional area to reduce the thermal effect.

In conclusion, although the laser power deposition on MgO: PPLN crystal is little, temperature variation is obvious. Crystal temperature distribution is closely related with the parameters mentioned above. An appropriate design of the laser parameters seems essential to optimize the laser thermal condition and improve the output laser quality.

Acknowledgements

This work was financially supported by the Fundamental Research Foundation of State Key Laboratory of Laser Interaction with Matter (Grant No. SKLLIM1711).

References

[1] W.R. Bosenberg, A. Drobshoff, J. Alexander, 93% pump depletion, 3.5-W continuous-wave, single resonant optical parametric oscillator, Opt. Lett. 21 (1996) 1336–1338.
[2] H.Y. Lin, X.G. Meng, Y.C. Xu, Parasitic oscillation in min-infrared optical parametric generator based on PPMgLN, Optik 124 (2013) 2511–2513.
[3] V. Ulvila, C.R. Phillips, L. Halonen, High-power mid-infrared frequency comb from a continuous-wave-pumped bulk optical parametric oscillator, Opt. Express 22 (2014) 10535–10543.
[4] H.Y. Lin, X. Liu, D. Sun, Continuous-wave eye-safe Nd:YVO4/PPMgLN intra-cavity optical parametric oscillator with shared resonator, Optik 138 (2017) 127–129.
[5] J. Liu, Q. Liu, X. Yan, High repetition frequency PPMgOLN mid-infrared optical parametric oscillator, Laser Phys. Lett. 7 (2010) 630–633.
[6] B. Wu, Y.H. Shen, S.S. Cai, Widely tunable high power O PO based on a periodically poled MgO doped lithium niobate crystal, Opt. Laser Technol. 39 (2007) 1115–1119.
[7] I.H. Bae, H.S. Moon, S. Zaske, Low-threshold single-resonant continuous-wave optical parametric oscillator based on MgO-doped PPLN, Applied Physics B-Laser and Optics 103 (2011) 311–319.
[8] J.J. Zondy, A. Douilley, A. Clairon, Thermal effects limitations in mid-infrared continuous wave optical parametric oscillators, J. Mater. Sci. Mater. Electron. 12 (2001) 451–460.
[9] S.T. Lin, Y.Y. Lin, Y.C. Huang, Observation of thermal-induced optical guiding and bistability in a mid-IR continuous-wave, singly resonant optical parametric oscillator, Opt. Lett. 33 (2008) 2338–2340.
[10] Y.F. Chen, Design criteria for concentration optimization in scaling diode end-pumped lasers to sigh powers: influence of thermal fracture, IEEE J. Quantum Electron. 35 (1999) 234–239.
[11] X.Y. Peng, L. Xu, A. Asundi, Power scaling of diode-pumped Nd:YVO4 laser, IEEE J. Quantum Electron. 38 (2002) 1291–1299.
[12] Y.S. Huang, H.L. Tsai, F.L. Chang, Thermo-optic effects affecting the high pump power end pumped solid lasers:modeling and analysis, Opt. Commun. 273 (2007) 515–525.
[13] Z. Mohammadzahery, M. Jandaghi, S. Alipour, Theoretical study on thermal behavior of passively switched microchip Nd:YAG laser, Opt. Laser Technol. 44 (2012) 1095–1100.
[14] X.H. Han, J.L. Li, Analytical solution of the transient temperature profile in gain medium of passively Q-switched microchio laser, Appl. Opt. 53 (2014) 7540–7550.
[15] O.A. Louchev, N.E. Yu, S. Kurimura, Thermal inhibition of high-power second-harmonic generation in periodically poled $LiNbO_3$ and $LiTaO_3$ crystals, Appl. Phys. Lett. 87 (2005) 131101.
[16] O.A. Louchev, N.E. Yu, S. Kurimura, Nanosecond pulsed laser energy and thermal field evolution during second harmonic generation in periodically poled LiNbO3 crystals, J. Appl. Phys. 98 (2005) 113103.
[17] X.H. Ma, Z.Y. Liu, R.Z. Zhang, Influences of laser thermal effect on second harmonic generation in periodically poled lithium niobate crystal, High Power Laser Part. Beams 23 (2011) 3302–3306.
[18] Y.T. Zhang, Q.Z. Qu, J. Qian, Thermal effect analysis of 1560nm laser frequency doubling in a PPLN crystal, Chinese J. Lasers 42 (2015) 0708002.
[19] J. Zheng, Y.Z. Li, P.W. Chen, Measurements of interfacial thermal contact conductance between pressed alloys at low temperature, Cryogenics 80 (2016) 33–43.